Critical and off-critical studies of the Baxter-Wu model with general toroidal boundary conditions

F. C. Alcaraz   and   J. C. Xavier

Departamento de Física

Universidade Federal de São Carlos

13565-905, São Carlos, SP, Brasil

Abstract

The operator content of the Baxter-Wu model with general toroidal boundary conditions is calculated analytically and numerically. These calculations were done by relating the partition function of the model with the generating function of a site-colouring problem in a hexagonal lattice. Extending the original Bethe-ansatz solution of the related colouring problem we are able to calculate the eigenspectra of both models by solving the associated Bethe-ansatz equations. We have also calculated, by exploring the conformal invariance at the critical point, the mass ratios of the underlying massive theory governing the Baxter-Wu model in the vicinity of its critical point.

1   Introduction

The Baxter-Wu model is the simplest non-trivial spin model with three-spin interactions. Its Hamiltonian is defined on a triangular lattice by

$$H = -J \sum_{<ijk>} \sigma_i \sigma_j \sigma_k, \tag{1}$$

1

where the sum extends over the elementary triangles, J is the coupling constant and $\sigma_i = \pm 1$ are Ising variables located at the sites. Historically this model was introduced by Wood and Griffiths in 1972 [1], as an example of a model exhibiting an order-disorder phase transition and not having a global up-down spin reversal symmetry. This model is self-dual [1, 2] with the same critical temperature as that of the Ising model on a square lattice. In 1973 Baxter and Wu [3] related the partition function of this model, in the thermodynamic limit, with the generating function of a site colouring problem on an hexagonal lattice. Solving this colouring problem through a generalized Bethe-ansatz they calculated the leading exponents [3] $\alpha = 2/3$, $\mu = 2/3$ and $\eta = 1/4$ of the Baxter-Wu model. The equality of these exponents with those of the 4-state Potts model [4-6] added to the fact that both models have the same four-fold degeneracy of the ground state, induce the conjecture that they share the same universality class of critical behaviour. This conjecture is interesting since contrary to the Baxter-Wu model the 4-state Potts model is exactly integrable only at its critical point. However from numerical studies of these models on a finite lattice it is well known that both models show different corrections to finite-size scaling (at the critical point). Whereas in the 4-state Potts models [7-10] these corrections are governed by a marginal operator, producing logarithmic corrections with the system size, which brings enormous difficulty to extract reliable results from finite-size studies of the model, this is not the case in the Baxter-Wu model [11-13].

Nowadays with the developments of conformal invariance applied to critical phenomena [13] the classification of different universality classes of critical behaviour becomes clear. Two models belong to the same universality class only if they share the same operator content, not only the leading critical exponents. The operator content of the 4-state Potts model was already conjectured from finite-size studies in its Hamiltonian formulation [14] and can be obtained by a $Z(2)$ orbifold of the Gaussian model in a special compactification radius (see [15] for a review). In this paper we numerically and analytically calculate the operator content of the Baxter-Wu model with several boundary conditions. Part of our numerical calculation was announced in [12]. In order to do this calculation we generalize the original Bethe-ansatz solution of the related site-colouring problem with periodic boundary condition. This is necessary because this solution only gives part of the eigenspectrum of the associated transfer matrix. We also extend our Bethe-ansatz solution in other cases where the site-colouring problem is not on a

periodic lattice. This extension enables us to obtain the operator content of this model and the Baxter-Wu model for more general toroidal boundary conditions. Our numerical study was done by numerically solving the Bethe-ansatz equations and the analytical work was done by studying these equations using standard techniques based on the Wiener-Hopf method [16].

We believe that beyond the Ising model the Baxter-Wu model is the simplest spin model that can be solved exactly for arbitrary temperatures. We explore this solution in order to obtain the mass spectrum of the massive theory describing fluctuations near the critical point.

The layout of this paper is as follows. In section 2 we introduce a site-colouring problem on an hexagonal lattice whose generating function is exactly related, in the bulk limit, with the Baxter-Wu model. Our construction is valid for some toroidal boundary conditions, generalizing the original construction [3] for periodic lattices. In section 3 we present the transfer matrix associated to the colouring problem and calculate its eigenvalues by the Bethe-ansatz. In section 4 the operator content of the Baxter-Wu model and the related site-colouring problem is obtained. The mass spectrum of the massive field theory governing the thermal and magnetic perturbations is calculated in section 5. Finally our conclusions are present in section 6 and the analytical calculation of some of the conformal dimensions of the site-colouring problem is presented in an appendix.

2   The Baxter-Wu model and the related site-colouring problem

In this section we relate the Baxter-Wu model with general toroidal boundary conditions with a *site-colouring problem* (SCP) on the hexagonal lattice. The construction presented here generalizes those presented by Baxter and Wu [3] for the periodic case.

Let us consider a triangular lattice with L (M) rows (columns) along the horizontal (vertical) direction, respectively. For convenience we take L as a multiple of 3, and decompose the lattice in three triangular sublattices formed by the points denoted by $\bigcirc$, $\square$ and $\triangle$ in Fig. 1. We attach at each site of a sublattice Ising variables $\{\sigma^\circ\}$, $\{\sigma^\square\}$ and $\{\sigma^\triangle\}$, and the Baxter-Wu model, with the Hamiltonian (1) is given in terms of the simplest three-body

interactions with one spin in each sublattice.

The model has a non-local $Z(2) \times Z(2)$ symmetry corresponding to the global change of variables in two of the sublattices, i.e.,

$$\sigma^\triangle \rightarrow a\sigma^\triangle \quad \sigma^\circ \rightarrow b\sigma^\circ \quad \sigma^\square \rightarrow ab\sigma^\square \quad (a = b = \pm 1).$$

This fact implies that at sufficiently low temperatures the model have a fourfold degenerate ground state. Creating, at low temperatures, domain walls connecting those different ground states we see that in fact the symmetry of those long-range excitations is $D(4)$, like in the 4-state Potts model. These reasonings suggest that critical fluctuations of both models are described in terms of the same quantum field theory. In order to do a detailed study of several sectors of this underlying field theory we consider the Baxter-Wu model with general toroidal boundary conditions compatible with its $Z(2) \times Z(2)$ symmetry:

$$\sigma_{i,j}^\triangle = a\sigma_{i+L,j}^\triangle \quad \sigma_{i,j}^\circ = b\sigma_{i+L,j}^\circ \quad \sigma_{i,j}^\square = ab\sigma_{i+L,j}^\square, \tag{2}$$

where $a, b = \pm 1$. In Fig.1 the simbols $\circ$, $\square$ and $\triangle$ denote the bordering sites which are related by (2) to the bulk ones (filled simbols). Imposing periodic boundary condition along the vertical direction the partition function of the model $Z_{L \times M}^{BW}$ can be written as

$$Z_{L \times M}^{BW} = Tr \left(\hat{T}_{(a,b)}^{BW} \right)^M, \tag{3}$$

where $\hat{T}_{(a,b)}^{BW}$ is the associated row-to-row transfer matrix. Its elements $\langle \sigma_1, ..., \sigma_N | \hat{T}_{(a,b)}^{BW} | \sigma_1', ..., \sigma_N' \rangle$ are given by the Boltzmann weights generated by the spin configurations $\{\sigma_1, ..., \sigma_N\}$ and $\{\sigma_1', ..., \sigma_N'\}$ of adjacent rows and are given by

$$\langle \sigma_1, ..., \sigma_N | \hat{T}_{(a,b)}^{BW} | \sigma_1', ..., \sigma_N' \rangle = \exp \left(K \sum_{j=1}^{L} \sigma_j' \sigma_{j+2}(\sigma_{j+1} + \sigma_{j+1}') \right), \tag{4}$$

with $K = \frac{J}{k_B T}$ and on the right side the appropriate boundary condition (a, b) is taken into account.

Following Baxter and Wu [3] we can relate $Z_{L \times M}^{BW}$ to the partition function or generating function $Z_{N \times M}^{SCP}$ of a SCP on an honeycomb lattice with $N = \frac{2L}{3}$

rows and M columns. In order to do this, it is convenient to define link variables $\{\lambda\}$ at the links of the hexagonal lattice formed by the sublattices $\circ$ and $\square$ (heavy lines in Fig.1). These variables are given by the product of the site variables at the ends of the link ($\lambda = \sigma^\square \sigma^\circ$). In terms of these new variables the Hamiltonian is given by

$$H = -J \sum_{i \in \triangle} \sigma_i^{\triangle}(\lambda_1 + \lambda_2 \cdots + \lambda_6), \tag{5}$$

where the summation is only over the sublattice $\triangle$ and $\lambda_1, \lambda_2, ..., \lambda_6$ are the link variables surrounding a given site variable $\sigma_i^{\triangle}$. Taking into account the boundary conditions (2) the partition function, in terms of these new variables, can be written as

$$Z_{L \times M}^{BW} = \sum_{\{\sigma^\triangle, \lambda\}} \prod_{\triangle} \left\{ \exp \left\{ K\sigma^{\triangle}(f_1\lambda_1 + f_2\lambda_2 + \cdots + f_6\lambda_6) \right\} \frac{1}{2}(1 + \lambda_1\lambda_2...\lambda_6) \right\},$$
$$\tag{6}$$

where the product extends over all the elementary hexagons formed by the sites in sublattices $\square$ and $\circ$, and surrounding a site variable $\sigma^\triangle$. The factor $\frac{1}{2}(1+\lambda_1\lambda_2...\lambda_6)$ in (6) is necessary since the variables $\{\lambda\}$ are not independent. The factors f_i ($i = 1, 2, ..., 6$) in (6) are constants defined on the links of the hexagonal lattice ($\square$-$\circ$) and depend on their relative location (see Fig. 1). If both ends of a link i (with corresponding variable λ_i) belongs to the bulk of the lattice ($\bullet$-$\blacksquare$) $f_i = 1$, if one of its ends is on the border ($\circ$-$\blacksquare$ or $\bullet - \square$) $f_i = ab$, and if both ends are on the border ($\circ$-$\square$) $f_i = a$. To proceed it is convenient [3] to rewrite the last product in (6), surrounding each lattice site $\triangle$ as

$$\frac{1}{2}(1 + \lambda_1\lambda_2...\lambda_6) = \sum_{\mu^\triangle = \pm 1} g(\lambda_1, \mu^\triangle)g(\lambda_2, \mu^\triangle) \cdots g(\lambda_6, \mu^\triangle), \tag{7}$$

where

$$g(\lambda, \mu) = 2^{-7/6}(\lambda + \mu + |\lambda - \mu|). \tag{8}$$

Substituting the expression (7) into equation (6) the partition function will be expressed in terms of a single sublattice $\triangle$ with site variables $\{\sigma^\triangle\}$ and $\{\mu^\triangle\}$, and link variables $\{\lambda\}$. Taking into account the boundary factors it is

5

straightforward to write

$$Z_{L \times M}^{BW} = \sum_{\{\sigma^\triangle, \mu^\triangle\}} \prod_{<i,j>} \left\{ \sum_{\lambda_{i,j}=\pm 1} \exp\left(K(\sigma_i^\triangle + \sigma_j^\triangle)\lambda_{i,j}\right) g(\lambda_{i,j}, \mu_i^\triangle) g(\lambda_{i,j}, \mu_j^\triangle) \right\},$$
(9)

where $<i,j>$ are links on the hexagonal lattice formed by the sublattices $\square$ and $\bigcirc$ (see Fig. 1). In order to derive (9) we are forced to restrict ourselves only to boundary conditions (2) where $a = b = \pm 1$. Fortunately this does not restrict our analysis since due to the $D(4)$ symmetry of the model, the eigenspectra of the transfer matrices with boundary condition $a \neq b$ and $a = b = -1$ are degenerate. Summing over $\{\lambda\}$ in (9) we obtain

$$Z_{L \times M}^{BW} = \sum_{\{\sigma^\triangle, \mu^\triangle\}} \prod_{<i,j>} w(\sigma_i^\triangle, \mu_i^\triangle; \sigma_j^\triangle, \mu_j^\triangle),$$
(10)

where

$$w(\sigma_i, \mu_i; \sigma_j, \mu_j) = 2^{-1/3} \left[\exp\left(K(\sigma_i + \sigma_j)\right) + \mu_i \mu_j \exp\left(-K(\sigma_i + \sigma_j)\right) \right].$$
(11)

Finally, following Baxter and Wu [3] we now associate the above partition function to the generating function of a SCP with 8 colours. We associate odd colours 1, 3, 5 and 7 at a given site $\triangle$ according to the values of the variables $(\sigma^\triangle, \mu^\triangle)$ attached at the site:

$$(++) \to 1 \quad (-+) \to 3 \quad (--) \to 5 \quad (++) \to 7.$$
(12)

The relation (11) tell us that links connecting colours 3,7 and 1,5 should be forbidden in the SCP. This constraint can be easily implemented [3] by introducing the even colours 2, 4, 6 and 8 on the sublattice $\bigcirc$, forming with the sublattice $\triangle$ an hexagonal lattice with $N = \frac{2}{3}L$ (M) sites in the horizontal (vertical) direction. The constraint is that all nearest-neighbour colours on this hexagonal lattice must differ by ± 1 (modulo 8). For $M \to \infty$, the partition function $Z_{L,M}^{BW}$ is then related to the generating function $Z_{N,M}^{SCP}$, given by

$$Z_{N,M}^{SCP} = \sum_{\{C\}} z_1^{n_1} z_2^{n_2} \cdots z_8^{n_8} = Z_{L,M}^{BW},$$
(13)

where $n_1, n_2, ..., n_8$ is the number of sites coloured with colour 1,2,...,8 in a given configuration C. The fugacities z_i ($i = 1, 2, ..., 8$) are obtained from

(11)

$$z_1 = z_3 = z_5 = z_7 = 2\sinh(4K),$$
$$z_2^{-1} = z_4 = z_6^{-1} = z_8 = \sinh(2K) \equiv t. \tag{14}$$

The critical point of the Baxter-Wu model and of the SCP is given by the self-dual point $t = t_c = 1$ [3]. Concerning the boundary conditions the relations are as follows. The $Z_{L,M}^{BW}$ with periodic boundary condition ($a = b = 1$ in (2)) is related with $Z_{N,M}^{SCP}$, also with periodic lattice. The boundary condition $a = b = -1$ in (2) is related to a boundary condition in the SCP such that if at site $(1, j)$ we have a colour variable $c_{1,j} = 1, 3, 5$ or 7 at site $(N + 1, j)$ the colour variable should be $c_{N+1,j} = 3, 1, 7$ and 5 respectively. We do not need to mention even colours since N is even (see Fig. 1).

3 The transfer matrix and the Bethe-ansatz of the SCP

In this section we derive the row-to-row transfer matrix of the SCP and generalize its Bethe-ansatz solution presented by Baxter and Wu [3]. The solution presented in [3], as we shall see, only gives part of the eigenspectra of the transfer matrix of the SCP, with periodic boundary conditions. Here we extend the solutions for the periodic case and also derive the Bethe-ansatz equations for the more general boundary condition

$$c_{i,j} = c_{i+N,j} + 2\kappa \pmod 8; \quad \kappa = 0, 1, 2 \text{ or } 3, \tag{15}$$

along the horizontal direction. The periodic case corresponds to $\kappa = 0$. Following [3], for a given configuration $\{c_{i,j}\}$ of colours on the hexagonal lattice, we say we have a dislocation on a given link of the lattice wherever the colour on the right end of the link is smaller (modulo 8) than that on the left end. In Fig. 2 we show two configurations with the corresponding dislocations (dotted lines) for a lattice with width $N = 4$. In Fig. 2a the lattice is periodic ($\kappa = 0$) and in Fig. 2b the boundary condition is given by (15) with $\kappa = 1$.

The generating function of the SCP can be written as

$$Z_{N,M}^{SCP} = Tr\left(\hat{T}_{(\kappa)}^{SCP}\right)^M, \tag{16}$$

where $\hat{T}^{SCP}_{(\kappa)}$ is the associated row-to-row transfer matrix. This transfer matrix has elements $\langle\{C\}|\hat{T}^{SCP}_{(\kappa)}|\{C'\}\rangle$ given by the product of the Boltzmann weights due to the colour configurations $\{C\} = \{c_1, c_2, .., c_N\}$ and $\{C'\} = \{c'_1, c'_2, ..., c'_N\}$ of two adjacent rows. If the configuration produced by $\{C\}$ and $\{C'\}$ contains only colours differing by ± 1 (modulo 8), we have

$$\langle\{C\}|\hat{T}^{SCP}_{(\kappa)}|\{C'\}\rangle = \prod_{i=1}^{N}(z(c_i)z(c'_i))^{1/2}, \tag{17}$$

with fugacities z_i defined in (14). On the other hand if the configuration does not satisfy this constraint, $\langle\{C\}|\hat{T}^{SCP}_{(\kappa)}|\{C'\}\rangle = 0$. It is simple to see that this requirement implies, for arbitrary values of κ in (15), the conservation of the number n of dislocations along the vertical direction. Consequently the Hilbert space associated to $\hat{T}^{SCP}_{(\kappa)}$ can be separated into block-disjoint sectors labelled by the values of n. The possible values of n depend on the boundary condition (15). For $\kappa = 0, 2$ (1, 3) they are even (odd), and are given by n_j, where

$$0 \le n_j = N - \kappa - 4j \le 2N \quad j = 0, \pm 1 \pm 2, ... \tag{18}$$

The colour configurations $\{C\}$ and $\{C'\}$, in a sector with n dislocations, can be conveniently expressed by the sets $(m; X) = (m; x_1, x_2, ..., x_n)$ and $(m'; X') = (m'; x'_1, x'_2, ..., x'_n)$, respectively. The odd numbers m and m' give the colour at the first site and the sets $X \equiv (x_1, x_2, ..., x_n)$ and $X' \equiv (x'_1, x'_2, ..., x'_n)$ give the position of the dislocations on the row. The sets X and X' should satisfy

$$1 \le x_1 \le x_2 \le \cdots \le x_n \le N \;\;, \;\; 1 \le x'_1 \le x'_2 \le \cdots \le x'_n \le N, \tag{19}$$

and should have no more than one repeated value of x or x' if they are odd, or more than three repeated values if they are even. In Fig. 2a we show the configurations $(m; X) = (1; 2, 3, 4, 4)$ and $(m'; X') = (3; 2, 2, 3, 4)$ which belong to the sector with $n = 4$ and periodic boundary condition. In Fig 2b we show the configurations $(m; X) = (1; 2, 3, 4)$ and $(m'; X') = (3; 2, 2, 2)$ belonging to the sector with $n = 3$ in the lattice with boundary condition $\kappa = 1$ in (15) and width $N = 4$. Two configurations $X = (x_1, x_2, ..., x_n)$ and $X' = (x'_1, x'_2, ..., x'_n)$ are connected through the operator $\hat{T}^{SCP}_{(\kappa)}$ if beyond (19)

$$\begin{aligned} x'_j &= x_j - 1, & \text{if } x_j \text{ odd} \\ x'_j &= x_j, x_j - 1, x_j - 2 & \text{if } x_j \text{ even.} \end{aligned} \tag{20}$$

In the case $x_i = x_{i+1}$ we have an additional constraint $x'_i \neq x'_{i+1}$. We should notice, for arbitrary boundary condition, the identification

$$X = (0, x_2, x_3, ..., x_n) = (x_2, x_3, ..., x_n, N). \tag{21}$$

The transfer matrix, in a given sector with n dislocations is now given by

$$\langle m, X | \hat{T}^{SCP}_{(\kappa)} | m', X' \rangle = z_{m+1}^{\frac{1-(-1)^\kappa}{4}} \prod_{j=1}^{n} w(m + x_j + x'_j - 2j), \quad w(m) = (z_m z_{m+1})^{1/2}, \tag{22}$$

if X and X' satisfy (19) and (20), and is zero otherwise. In the sector with n dislocations the eigenvectors $\psi^{(n)}$ of $\hat{T}^{SCP}_{(\kappa)}$, with eigenvalue Λ can be written as

$$\psi^{(n)} = \sum_{\{m,X\}} z_{m+1}^{-\frac{1-(-1)^\kappa}{8}} f_m(x_1, x_2, \cdots, x_n) | m; X \rangle, \tag{23}$$

where the summation is restricted to the configurations with n dislocations, and $f_m(x_1, x_2, \cdots, x_n)$ are unknown amplitudes. The eigenvalue equation for $\hat{T}^{SCP}_{(\kappa)}$ is given by

$$\sum_{X'}^{*} \left(\prod_{j=1}^{n} w(m + x_j + x'_j - 2j) \right) f_{m+2}(X') = \Lambda f_m(X), \tag{24}$$

where the asterisk indicates that X and X' satisfy the conditions (19) and (20). The relation (21) implies that in (24) the amplitudes having $x'_1 = 0$ should be replaced by the boundary condition

$$f_{m+2}(0, x'_2, x'_3, \cdots, x'_n) = z_{m+1}^{\frac{1-(-1)^\kappa}{4}} f_m(x'_2, x'_3, \cdots, x'_n, N). \tag{25}$$

Due to the values of the fugacities (14) it is simple to see that $\hat{T}^{SCP}_{(\kappa)}$, besides conserving the number of dislocations, also has an additional $Z(2)$ symmetry (eigenvalues $\epsilon = \pm 1$), since adding 4 (modulo 8) to all colours in a given configuration does not change its weight in the generating function, that is

$$f_{m+4}(X) = \epsilon f_m(X). \tag{26}$$

Following Baxter and Wu [3] we assume the following Bethe-ansatz for the amplitudes

$$f_m(X) = \sum_P a(P) \phi_{P_1}(m - 2, x_1) \cdots \phi_{P_n}(m - 2n, x_n), \tag{27}$$

9

where the summation is over all the $n!$ permutations $P = \{P_1, P_2, ..., P_n\}$ of integers $\{1, 2, ..., n\}$. We require the existence of n wave numbers k_j ($j = 1, 2, ..., n$) and signs ϵ_j ($j = 1, 2, ..., n$) such that

$$\phi_j(m, x) = \epsilon_j \phi_j(m + 4, x) = \begin{cases} a_{j,m} \exp(ik_j x), & x \text{ odd} \\ b_{j,m} \exp(ik_j x), & x \text{ even}. \end{cases} \quad (28)$$

Observe that the $Z(2)$-parity eigenvalue of the wave function is given by $\epsilon = \prod_{j=1}^{n} \epsilon_j$, and it is even or odd depending on the numbers of negative values of ϵ_j. The Bethe-ansatz solution presented by Baxter and Wu [3] only gives the symmetric eigenvalues ($\epsilon = 1$), for periodic boundary conditions ($\kappa = 0$). We can follow the same procedure as in [3] in order to derive the Bethe-ansatz equations. We have to consider various possible choices of X to determine the eigenvalue Λ.

Firstly let us consider the case where all dislocations are located at distinct positions, i.e., $x_1 \neq x_2 \neq \cdots \neq x_n$. Eq. (24) is then replaced by

$$\sum_{x'} w(m + x + x')\phi_j(m + 2, x') = \lambda_j \phi_j(m, x), \quad j = 1, ..., n, \quad (29)$$

where we have denoted

$$\Lambda = \lambda_1 \cdots \lambda_n. \quad (30)$$

Actually Eq. (29) represents two equations corresponding to x odd or even and can be written as

$$T_{j,m+2} V_{j,m+2} = \lambda_j V_{j,m}, \quad (31)$$

where

$$T_{j,m+2} = \begin{pmatrix} 0 & \alpha_{j,m+1} \\ \alpha_{j,m-1} & A_{j,m} \end{pmatrix}; \quad V_{j,m} = \begin{pmatrix} a_{j,m} \\ b_{j,m} \end{pmatrix} \quad (32)$$

with

$$\alpha_{j,m} = w(m) \exp(-ik_j); \quad A_{j,m} = w(m) + w(m - 2) \exp(-2ik_j). \quad (33)$$

Using the fact that

$$\begin{pmatrix} a_{j,m-2} \\ b_{j,m-2} \end{pmatrix} = \epsilon_j \begin{pmatrix} a_{j,m+2} \\ b_{j,m+2} \end{pmatrix},$$

it is simple to see that λ_j can be obtained from the eigenvalue equation

$$(T_{j,m} T_{j,m+2}) V_{j,m+2} = \lambda_j^2 \epsilon_j V_{j,m+2}.$$

10

Solving for the eigenvalues of $T_{j,m}T_{j,m+2}$ we see that λ_j does not depend on the value of m (as it is expected) and satisfies

$$\lambda_j^4 - \epsilon_j \lambda_j^2 [\exp(-i4k_j) + \Delta \exp(-2ik_j) + 1] + \exp(-4ik_j) = 0, \qquad (34)$$

where $\Delta = t + 1/t$. The solution of (34) is given by $\lambda_j = \sqrt{\epsilon_j} \exp(e_j^{(s_j)} - ik_j^{(s_j)})$, with

$$e_j^{(s_j)} = 1/2 \ln \left(x_j + s_j \sqrt{x_j^2 - 1} \right), \quad x_j = \cos(2k_j^{(s_j)}) + \Delta, \qquad (35)$$

and $s_j = \pm 1$. Equation (31) gives the relations

$$a_{j,m+2} = \epsilon_j \alpha_{j,m-1} b_{j,m}/\lambda_j,$$
$$b_{j,m+2} = \sqrt{\epsilon_j} \Omega_{j,m} b_{j,m},$$
$$a_{j,m} = \sqrt{\epsilon_j} \alpha_{j,m+1} \Omega_{j,m} b_{j,m}/\lambda_j, \qquad (36)$$

where

$$\Omega_{j,m} = \epsilon_j \sqrt{\epsilon_j} A_{j,m}^{-1} (\lambda_j - \epsilon_j \alpha_{j\,m-1}^2/\lambda_j^{-1}). \qquad (37)$$

It is important to verify that $\Omega_{j,m+2}\Omega_{j,m} = 1$, so that at $t = t_c = 1$, $\Omega_{j,m}^2 = 1$.

Secondly let us consider the case where two even dislocation positions x coincide. For convenience suppose $x_1 = x_2 = x$ (even). If we require that the ansatz (27) satisfies (24) with eigenvalue given by (30) and (35) the equation

$$\sum_{x_1',x_2'}^{*} w(m+x+x_1'-2)w(m+x+x_2'-4)f_{m+2}(x_1',x_2') = \lambda_1\lambda_2 f_m(x,x), \quad (38)$$

must be fulfilled, where

$$f_{m+2}(x_1, x_2) = a(1,2)\phi_1(m, x_1)\phi_2(m-2, x_2) + a(2,1)\phi_2(m, x_1)\phi_1(m-2, x_2),$$
$$(39)$$

and the asterisk in Eq. (38) indicates summation over the possible configurations $(x_1', x_2') = (x-2, x-1), (x-2, x), (x-1, x)$. Using (28), (32), (34) and (36) in (38) we obtain after some algebra (the same algebra as in [3]), that the ratio

$$\tilde{B}_{12} \equiv \frac{a(1,2)}{a(2,1)} = -\frac{\sqrt{\epsilon_2}}{\sqrt{\epsilon_1}} \frac{\cosh(e_1^{(s_1)} + ik_2)}{\cosh(e_2^{(s_2)} + ik_1)} = \frac{\sqrt{\epsilon_2}}{\sqrt{\epsilon_1}} B_{12}, \qquad (40)$$

is also independent of m

11

More generally in order for the Bethe-ansatz (27) to work we should have

$$\tilde{B}_{jl} \equiv \frac{a(...,j,l,...)}{a(...,l,j,...)} = -\frac{\sqrt{\epsilon_l}}{\sqrt{\epsilon_j}} \frac{\cosh(e_j^{(s_j)} + ik_l)}{\cosh(e_l^{(s_l)} + ik_j)} = \frac{\sqrt{\epsilon_l}}{\sqrt{\epsilon_j}} B_{jl}, \qquad (41)$$

for all permutations of adjacent elements in $a(P)$. Following the same steps as in [3] it can be proved that equations (41) are enough to ensure the effectiveness of the ansatz (27) in the case of triple coincidence of dislocations. In order to complete the solution we still need to fix the wave numbers $\{k_1, k_2, ..., k_n\}$. As usual this is done by inserting (27) in the boundary condition (25),

$$\sum a(P_1, ..., P_n)\phi_{P1}(m,0)\left[\phi_{P_2}(m-2, x_2) \cdots \phi_{P_n}(m-2n+2, x_n)\right] = z_{m+1}^{\frac{1-(-1)^\kappa}{4}}$$
$$\sum a(P_2, ..., P_n, P_1)\left[\phi_{P_2}(m-2, x_2) \cdots \phi_{P_n}(m-2n+2, x_n)\right]\phi_{P_1}(m-2n, N),$$
$$(42)$$

where in the right-hand side a circular shift on P was done. This equation is fulfilled if we require that

$$a(P_1, P_2, ..., P_n)\phi_{P_1}(m,0) = z_{m+1}^{\frac{1-(-1)^\kappa}{4}} a(P_2, P_3, ..., P_n, P_1)\phi_{P_1}(m-2n, N). \quad (43)$$

Using (38), (36) and (41) we then obtain

$$\exp\left(iNk_j\right) = -(-1)^{n_-}\rho_{m,j}^{(\kappa)} \prod_{l=1}^{n} B_{jl}, \quad j = 1, 2, ..., n \qquad (44)$$

where

$$n_- = \text{int}[\frac{1}{2}\sum_i \delta_{\epsilon_i,-1}] \quad \text{and} \quad \rho_{m,j}^{(\kappa)} = \left(\frac{\Omega_{j,m}^2}{z_{m+1}}\right)^{\frac{1-(-1)^\kappa}{4}}. \qquad (45)$$

Actually we have in (44) two distinct sets of equations, a first one for $m = 1$ and $m = 5$ and a second one for $m = 3$ and $m = 7$. These sets must be solved simultaneously for the validity of the Bethe-ansatz (27). From Eqs. (14) and (33)-(37) we verify that those equations degenerate ($\rho_{m,j}^{(\kappa)} = 1$, $m = 1, 3, 5, 7; j = 1, 2, ..., n$) in the following cases: (a) $\kappa = 0$ or 2 for arbitrary values of temperatures t, (b) $\kappa = 1$ or 3 only at the critical temperature $t = t_c = 1$. In both cases the Bethe-ansatz equations are given by

$$\exp(-iNk_j) = -(-1)^{n_-}\sqrt{\epsilon} \prod_{l=1}^{n} B_{jl}, \quad \epsilon = \pm 1 \qquad (46)$$

with $B_{j,l}$ and n_- given by (41) and (45), respectively. For a given value of $\epsilon = \pm 1$ the prefactor $\delta_- = (-1)^{n_-}$, in Eq. (46), may be positive or negative depending on the particular choice of the set $\{\epsilon_1, ..., \epsilon_n\}$. If n is even these two choices are equivalent. The solution of both equations are the same except that one of the quasi-moments differs by the value π (mod 2π). However if n is odd the situation is different, and we should consider both equations. Their solution gives us independent wave-functions.

4 The operator content of the Baxter-Wu model and the SCP

In this section, by exploiting the conformal invariance at the critical point, we are going to derive the operator content of the Baxter-Wu model and the SCP. The conformal anomaly c and anomalous dimensions $(x_1, x_2, ...)$ are obtained in a standard way from the finite-size behaviour of the eigenspectra of the associated transfer matrix, at the critical temperature. If we write $T = \exp(-\hat{H})$, then in a strip of width L with periodic boundary conditions the ground-state energy, $E_0(L)$, of $\hat{H}$ behaves for large L as [17]

$$\frac{E_0(L)}{L} = \epsilon_\infty - \frac{\pi c v_s}{6L^2} + o(L^{-2}), \tag{47}$$

where ϵ_∞ is the ground-state energy, per site, in the bulk limit. Moreover, for each operator O_α with dimension x_α there exists a tower of states in the spectrum of $\hat{H}$ with eigenenergies given by [13, 18]

$$E_{m,m'}^\alpha(L) = E_0 + \frac{2\pi v_s}{L}(x_\alpha + m + m') + o(L^{-1}), \tag{48}$$

where $m, m' = 0, 1, 2, \dots$. The factor v_s appearing in the last two equations is the sound velocity and has unit value for isotropic square lattices. We can calculate directly the higher eigenvalues of $\hat{T}_{(a,b)}^{BW}$ and $T_{(\kappa)}^{SCP}$ of our model by a numerical diagonalization, using for example the power method. However since these matrices are not sparse and have dimension 2^L, for a horizontal width L, we cannot compute the eigenspectra by numerical diagonalization methods for $L > L_0 \sim 18$ in the case of the Baxter-Wu model.

Instead of a direct calculation we can explore the relation (13) among the Baxter-Wu model and the SCP, and solve numerically the associated Bethe ansatz equations derived in section 3. If we write $T = \exp(-\hat{H})$ for both models, the relation (13) implies

$$Tr(e^{-MH_L^{BW}}) = Tr(e^{-MH_N^{SCP}}), \tag{49}$$

where $N = \frac{2L}{3}$. Its is important to observe that although H_L^{BW} and H_N^{SCP} have the same dimension 2^L they may have different eigenvalues. Indeed that is the case, specially if $t \neq t_c = 1$ as we can verify by a brute force diagonalization of these transfer matrices on small lattices. In order to present our results let us rewrite the Bethe-ansatz equations (46) in a convenient form. We are going to choose the prefactor $\delta_- = (-1)^{n_-} = 1$, since as we discussed in the last section, if n is even all the energies can be obtained from a given choice of δ_-, and for n odd the energies obtained by different choices of δ_- are complex-conjugate pairs. The eigenvalues $E_n^{\{s_j\}}$ of H_N^{SCP} in the sector with n dislocations are given by

$$E_n^{\{s_i\}} = -\frac{N}{4}\ln(16t^2(1+t^2)) - \sum_{j=1}^{n}(e_j^{(s_j)} - ik_j^{(s_j)}), \qquad (50)$$

where
$$e_j^{(s_j)} = 1/2\ln\left(x_j + s_j\sqrt{x_j^2 - 1}\right), \quad x_j = \cos(2k_j^{(s_j)}) + t + 1/t, \qquad (51)$$

with $1 = s_1 = s_2 = \ldots = s_{n-l} = -s_{n-l+1} = \ldots = -s_n$, and $l = 0, 1, ..., n$ fixed. The quasi-momenta $\{k_j^{(s_j)}\}$ are obtained by solving the equations

$$\exp\left(iNk_j^{(s_j)}\right) = -\sqrt{\epsilon}\prod_{p=1}^{n}\left(\frac{\cosh(e_j^{(s_j)} + ik_p^{(s_p)})}{\cosh(e_p^{(s_p)} + ik_j^{(s_j)})}\right); \quad j = 1, 2, ..., n, \qquad (52)$$

where $\epsilon = 1$ ($\epsilon = -1$) gives the even (odd) part of the eigenspectrum, with respect to the $Z(2)$ symmetry of the SCP discussed in the last section. Strictly speaking these energies may only give part of the eigenspectra, since the completeness of the Bethe-ansatz solution presented in the last section is an open question. Numerically we have studied these equations extensively for lattice sizes up to $N \sim 200$ and part of our results at $t = t_c = 1$ were presented in [12]. For example, the ground-state energy for H_N^{SCP} corresponding to the boundary conditions $\kappa = 0, 1, 2$ and 3 given in (15) belongs to the sector where $n = N - \kappa$, $s_1 = s_2 = \cdots = s_n = 1$ and $\epsilon = 1$. In table 1 we present these ground-state energies, per site, for $\kappa = 0, 1$ and 2 ($\kappa = 3$ is degenerate with $\kappa = 1$). The conformal anomaly is obtained by using (47). The bulk energy $\epsilon_\infty^{SCP} = -\frac{3}{4}\ln 6$ can be obtained from the exact solution in the bulk limit [3] and the sound velocity $v_s^{SCP} = \sqrt{3}/3$, can be inferred from (48) and an overall analysis of the dimensions appearing in the model. With these values the ground-state energy (first column in table 1) gives us the estimators $c(N)$ presented in table 2. As expected the conformal anomaly is $c = 1$, as for the 4-state Potts model. The direct calculation of the eigenspectra of H^{SCP} and H^{BW} for small chains shows us that although the eigenspectra of both models is not the

14

same, several eigenvalues coincide. This is the case for the ground-state. Consequently by using the bulk limit value [3] $\epsilon_\infty^{BW} = -\frac{1}{2}\ln 6$, and the sound velocity $v_s^{BW} = \sqrt{3}/2$, we obtain the expected value $c = 1$ for the Baxter-Wu model.

The dimensions defining the operator content of the model are obtained from the large-N behaviour of the energies of excited states. Let us concentrate on the SCP. The Bethe-ansatz equations (52) are the same for all boundary conditions, specified by κ (0,1,2 and 3) in (15), only the allowed values of n, given by (18) depend on the particular value of κ. Using (48), the finite-size sequences for some dimensions are shown in table 3. In this table $x_j^\epsilon(N-n,l)$ are the estimators of the dimensions associated to the jth lowest eigenenergy in the eigensector labelled by n and ϵ. The values of l used in (50)-(52) to obtain the corresponding energies are also shown. The numerical solution of (50)-(52) was done by the Newton type method. The roots $\{k_j\}$ for all the solutions that we obtained are real. Although we cannot discard this possibility for higher states, we do not find any string-type solution. The numerical solution of (50)-(52) is not easy for $N \sim 200$ due to numerical instabilities, and some tricks are necessary. In most cases we solve initially these equations for small values of t, where a good guess can be given, and use the solution obtained as the initial guess for a larger value of t. We repeat this process up to $t = t_c = 1$. As a result of our extensive calculation of the eigenspectra of H^{SCP} we arrive at the following conjecture. Namely, the dimensions of primary operators in a given sector labelled by $n = N + \kappa + 4j$ ($j = 0, \pm1, \pm2, ...$) of the H^{SCP} with boundary condition κ (0,1,2 or 3) are given by

$$x_{p,q} = \frac{1}{2}(4p^2 + \frac{q^2}{4}), \quad p = j - \frac{\kappa}{4}, \quad q = 0, \pm1, \pm2, ... \tag{53}$$

In obtaining (53), the value of E_0 in (48) is the value of the ground-state energy for the periodic ($\kappa = 0$) SCP. Moreover the number of descendants with dimensions $x_{p,q}^{(\kappa)} + m + m'$ ($m, m \in Z$) is given by the product of two independent Kac-Moody characters. This allows, by using (47) and (48), to write the generating function $Z_{N \times M}^{SCP}(\kappa)$ of the SCP with boundary condition κ, up to order $\exp(-M/N)$ ($M, N \to \infty$) as

$$Z_{N \times M}^{SCP}(\kappa) = \exp(-e_\infty^{SCP}MN)z^{1/12}\Theta^2(z) \sum_{p \in (Z - \kappa/4)} \sum_{q \in Z} z^{\frac{1}{2}(4p^2 + \frac{1}{4}q^2)} \tag{54}$$

where

$$z = \exp(\frac{2\pi N}{M}v_s^{SCP}) \qquad \Theta(z) = \prod_{n=0} (1 - z^n)^{-1}. \tag{55}$$

Since the Bethe-ansatz roots $\{k_j\}$ of (52) are real numbers, we can apply analytical methods [21-24] based on the Wiener-Hopf method to obtain the finite-size cor-

rections of the eigenenergies. We calculate the finite-size corrections of the lowest eigenenergies in the sector with n dislocations and parity ϵ. Since these calculations are rather technical we present them in appendix A for the interested reader. These analytical results are in agreement with the conjecture (53), obtained from the numerical solutions of (50)-(52).

Let us return to the Baxter-Wu model. Consider initially the model with periodic boundary conditions ($a = b = 1$ in (2)). Comparing the eigenspectra of $\hat{T}_{+,+}^{BW}$ and $\hat{T}_{(0)}^{SCP}$, obtained by a direct diagonalization on small lattices, we verify that many of the dimensions $x_{p,q}^{(0)}$ appearing in (53) are absent. For example, the energies producing the estimator $x_4^+(0,1)$ in the 5th row of table 3 only appear in $T_{(0)}^{SCP}$. Following for large lattices the energies which are exactly related in both models we verified that the lower dimensions in the Baxter-Wu model, with periodic boundary condition, are given by $x = 0, \frac{1}{8}, \frac{1}{2}, \frac{9}{8}, \ldots$, and appear with degeneracy $d_x = 1, 3, 1, 9, \ldots$, respectively. Due to its $D(4)$ symmetry the Baxter-Wu model has the same eigenspectra for the non-periodic boundary conditions given in (2), i.e., $(a, b) \neq (+, +)$. We have shown, at the end of section 3, that the partition function in these cases is exactly related with a SCP with boundary conditions not included in (15). Actually the application of the Bethe-ansatz in this case, if possible, is more difficult since the number of colours in a row is not a good quantum number anymore. However at $t = t_c = 1$ our direct calculations of the eigenspectra on small chains shows that there exist exact coincidences between the eigenvalues of $\hat{T}_{(-,-)}^{BW}$ and those of $\hat{T}_{(\kappa)}^{SCP}$, which are given by the Bethe-ansatz equations (50)-(52). These coincidences enable us to verify that the lower dimensions of the Baxter-Wu model with boundary condition $(a, b) \neq (+, +)$ in (2) are given by $x = 1/8, 1/2, 10/16, \ldots$ and appear with degeneracy $d_x = 1, 1, 4, \ldots$ These are the same dimensions reported in [14] for the 4-state Potts model with antiperiodic boundary condition. These results supplemented with the global eigenspectrum calculated for small systems, indicate that the operator content of the Baxter-Wu model is the same as that of the 4-state Potts model [14] and is given in terms of a $Z(2)$ orbifold [15] of the Gaussian model.

Before closing this section, since we have calculated the eigenspectra of H^{BW} and H^{SCP} for large lattices we can also calculate the dimensions of the operators responsible for the corrections to finite-size scaling in both models. Since these calculations were already presented earlier (see Eqs.(11)-(12) and Table 3 in [12]), we only mention that $x_\gamma = 4$ is the lowest dimension of the operator responsible for the finite-size deviations of the critical behaviour. This means that relations (47) and (48) have corrections which are power-like with the system size L. These corrections are like those of the Ising model and different from those of the 4-

16

state Potts model. This explains why the finite-size studies of the Baxter-Wu model have good convergence, in contrast with the 4-state Potts model, where the operator responsible for these corrections is marginal ($x_\gamma = 2$) producing logarithmic behaviour with the system size.

5 The off-critical properties of the Baxter-Wu model

The Baxter-Wu model and the SCP have a massive spectra at $t \neq t_c = 1$. A continuum field theory describing the long-distance physics in this phase can be obtained in the neighborhood of the perturbing thermal parameter $\delta = t - t_c \lesssim 0$. Such a field theory will be massive and the masses can be estimated from the finite-size behaviour of the eigenspectra of $H = -\ln \hat{T}$. We can calculate the mass spectrum by applying the scheme proposed by Sagdeev and Zamolodchikov [23] in the study of the Ising model under the influence of magnetic perturbations. According to this scheme we should initially calculate the finite-size corrections of the zero-momenta eigenenergies $E_k(\delta, L)$, $k = 0, 1, 2, ...$, at the conformal invariant critical point $\delta = 0$. From our analysis presented in the last section these corrections are governed mainly by an irrelevant operator with dimension $x_\gamma = 4$ and have integer power-law behaviour with the system size L. According to conformal invariance [18] $E_k(\delta, L)$ should behave as

$$E_k(L) = e_\infty L + \frac{2\pi v_s}{L}\left(x_k - \frac{c}{12}\right) + a_{k,1}L^{-3} + a_{k,2}L^{-5} + \cdots, \qquad (56)$$

where x_k is the conformal dimension associated to E_k and $a_{k,i}$ ($i = 1, 2, ...$) are L-independent factors. According to the scheme of [23], if the perturbed operator which produces the massive behaviour has dimension y, we should calculate the eigenspectra in the asymptotic regime $\delta \to 0$, $L \to \infty$, with

$$X = \delta^{\frac{1}{2-y}}L \qquad (57)$$

kept fixed. In this regime (56) is replaced by

$$E_k(\delta, L) = e_\infty L + \delta^{\frac{1}{2-y}}F_k(X) + a_{k,1}\delta^{\frac{3}{2-y}}G_k(X) + a_{k,2}\delta^{\frac{5}{2-y}}H_k(X) + \cdots . \qquad (58)$$

The masses of the continuum field theory are obtained from the large-X behaviour of the functions [23] $F_k(X)$, and are given by

$$m_k \sim F_k(X) - F_0(X), \qquad (59)$$

17

where $F_0(X)$ is associated in (58) with the ground-state energy.

In the present application, the thermal fluctuations are produced by the energy operator, which has dimension $y = x_\epsilon = 1/2$. Since we are going to calculate the eigenenergies of the Baxter-Wu model by exploiting its connection with those of the SCP, it is important to compare their eigenspectra for small lattice sizes. In table 4 we represent for $t < t_c$ ($T > T_c$) the relative location in the eigenspectra of the lower zero-momentum energies of both models. The eigenenergies in the same line are exactly degenerate on the finite lattice. In this table we also show the parity-quantum number $\epsilon \pm 1$, of the eigenenergies of H^{SCP}.

It is important to mention that although the Baxter-Wu model and the SCP are exactly related, the parameter t has quite a different effect in both models. In the case of the Baxter-Wu model it drives the system from an ordered phase ($T < T_c$, $t > t_c = 1$) to a disordered phase ($T > T_c$, $t < t_c = 1$). On the other hand, as we can see form (14), in the SCP it drives the model from an ordered phase rich in colours 4 and 8 ($t > t_c = 1$) to another ordered phase rich in colours 2 and 6 ($t < t_c = 1$). This fact implies that even for $T > T_c$ we should have in the SCP an infinite set of states, including the ground state, that degenerate exponentially with the system size ($E_n - E'_n \sim \exp(-aL)$), which certainly is not the case for the Baxter-Wu model in its disordered phase. In table 4 the pair of levels E_i^{SCP} and E_{i+1}^{SCP} ($i = 0, 2$ and 4) degenerate exponentially. Baxter and Wu [3] in their original calculation of the exponent α of the Baxter-Wu model used the excited energy $E_2^{SCP}(\epsilon = 1)$, instead of $E_3^{SCP}(\epsilon = -1) = E_1^{BW}$. However, as we mentioned, these energies become exponentially degenerate with system size, not changing their exact result $\alpha = 2/3$.

Exploring the correspondences presented in table 4 and using (57)-(59) we can calculate the mass ratios of the underlying massive field theory governing the Baxter-Wu model for $T \neq T_c$. They are calculated from the asymptotic regime $X \to \infty$ of the finite-size sequences

$$R_k(X, L) = \frac{F_k(X, L) - F_0(X, L)}{F_1(X, L) - F_0(X, L)} \to \frac{m_k}{m_1}. \tag{60}$$

The functions $F_k(X, L)$ are obtained by using in (58) the finite-size sequences of the zero-momentum states ($k = 0, 1, 2...$). The exact degeneracy of E_1^{BW} (see table 4) implies the first mass m_1 is triple generated. From the equality $E_2^{BW} = E_4^{SCP}$ we can calculate the second mass m_2 by solving the Bethe-ansatz equations derived in section 3 for the SCP. Unfortunately, although trying hard, we were not able to find the Bethe-ansatz roots that would correspond to this energy. However, applying the Lanczos method directly in H^{SCP} we calculate this eigenenergy up to $L = 21$, in the Baxter-Wu model. In table 5 we show the estimators $R_2(X, L)$

18

obtained by using in (58)-(60) $L = 15, 18$ and 21. These results are consistent with the conjecture $m_2 = \sqrt{3}m_1$. In the case of mass m_3 our results are more precise since we were able to calculate $E_3^{BW} = E_6^{SCP}(\epsilon = 1)$ for lattice sizes up to $L=150$, by solving the Bethe-ansatz equations (50)-(52). In table 6 we show the estimator $R_3(X, L)$ for some values of X, obtained by using in (58)-(60) $L = 144, 147$ and L=150. These results show clearly that $m_3 = 2m_1$. The numerical analysis of other higher energies in the spectrum shows that a continuum starts at m_3.

The mass ratios we obtained should be the same as those of the 4-state Potts model, since we expect both models share the same universality class of critical behaviour. In fact they coincide with the masses previously conjectured [24] for the 4-state Potts model and are also given by the masses of a sine-Gordon model [25] at a special coupling, i. e.,

$$m_{i+1} = m_1 \sin(\frac{\pi}{6}i), \quad i = 1, 2, 3. \tag{61}$$

To conclude this section we mention that we also studied the effect of magnetic perturbations in the Baxter-Wu model. This was done by calculation of the eigenspectra of $\hat{T}_{L,M}^{BW}$ with the addition of an external magnetic field h. In this case $\delta = h$ and $y = 1/8$ in (58), and the masses we obtained are consistent with those reported in [26] for the 4-state Potts model. However our results in this case, specially for larger masses, lack precision because we had to calculate directly the eigenspectrum of $\hat{T}_{L,M}^{BW}$, since the equivalence with the SCP presented in section 2 is not valid anymore and unlike $\hat{T}_{N,M}^{SCP}$ this matrix is not sparse.

6 Conclusions and Comments

The operator content of the Baxter-Wu model was calculated for several boundary conditions by exploiting the conformal invariance of the infinite system at the critical point. Our results are calculated analytically and numerically for very large lattice sizes. This was possible due to the relation between the Baxter-Wu model and the SCP. Actually we showed that the partition functions of both models are exactly related for several boundary conditions (see section 2) and we were able to extend the original Bethe-ansatz solution [3] for most of these boundaries (see section 3)

The operator content of the SCP with several toroidal boundary conditions (see (53)-(55)) is the same as those of a Gaussian model with dimensions [27]

$$x_{n,m} = gn^2 + \frac{m^2}{4g}, \tag{62}$$

19

where $g = 1/8$ is the compactification radius and $n, m \in Z$ are the vorticity and spin-wave number, respectively. However only part of the eigenspectra of both models coincide. Our analysis (section 4) shows that the dimensions of the Baxter-Wu model, for several boundary conditions are given by a $Z(2)$ orbifold of the above Gaussian model. This operator content coincides with the 4-state Potts model, indicating that indeed both models share the same universality class of critical behaviour. It is interesting to remark that whereas for the SCP the operator content is given in terms of characters of the Kac-Moody algebra, in the Baxter-Wu model the characters are those of the Virasoro algebra.

On the other hand a similar exact relation as that between the SCP and the Baxter-Wu model also exists between the 4-state Potts model and the 6-vertex model at its isotropic point ($\gamma = 0$), or equivalently the quantum XXX chain (anisotropy $\gamma = 0$). The operator content of this model is given by a combination of the dimensions given in (62) but with $g = 1/2$. In the 6-vertex model, or XXZ chain, the point where $g = 1/8$ corresponds to the anisotropy $\gamma = 3\pi/4$, and is the so-called Kosterliz-Thouless point. This implies that exactly at the critical point ($L \to \infty, T = T_c$) the Baxter-Wu model and the 4-state Potts model are governed by the same conformal theory, but deviations from the critical point, like for example the finiteness of the lattice, will be governed by an effective Gaussian model with different compactification radius. It is known [8] that in the case of the 6-vertex model or XXZ chain the finite-size corrections are ruled mainly by the operator with dimension $x_{0,2}$ in (62) besides the descendant of identity operator with dimension 4. This implies the appearance of logarithmic corrections, with the system size, at $g = 1/2$ since $x_{0,2} = 2$ and the corresponding operator responsable for such corrections is marginal. On the other hand at $g = 1/8$ we only have integer power-law corrections with the system size, since in this case the operator with dimension 4 dominates the finite-size correction. This explains why although the Baxter-Wu model and the 4-state Potts model are given by the same $Z(2)$ orbifold of a Gaussian theory, they show quite different behaviour at finite lattices.

In section 5 we calculated the mass spectrum of the underlying field theory governing the Baxter-Wu model around its critical point. In the case of thermal perturbations we obtained the masses given in (61) which are the same as those of the 4-state Potts model [24] and are also the masses of a special point of a massive sine-Gordon field theory [25]. Finally in the case of magnetic perturbation our numerical results, although poorer, are consistent with the same masses reported earlier for the 4-state Potts model [26].

Acknowledgments

Appendix

A Analytic calculation of the leading finite-size corrections

In this appendix we calculate analytically the leading finite-size corrections for some of the eigenenergies of the SCP at the critical point $t = t_c = 1$. We will calculate the finite-size corrections of the lowest energies $E_n(\epsilon)$ of the Hamiltonian, $H^{SCP} = -\ln \hat{T}_{SCP}$, in the sector with n dislocations and $Z(2)$-colour parity ϵ ($n = 0, 1, 2, ...; \ \epsilon = \pm 1$). Since the associated roots of the Bethe-ansatz equations are real numbers our analytical calculations are based on the method pioneered by de Vega and Woynarovich [19] and Hamer [20] and refined by Woynarovich and Eckle [21] (see also [22]). In order to apply this method it is convenient to change the variables $\{k_1, k_2, ..., k_n\}$ appearing in (46) into new variables $\{u_1, u_2, ..., u_n\}$ so that $B_{j,l}$ become a function of the difference $u_j - u_l$. This was done by Baxter and Wu [3] for arbitrary temperatures and $B_{j,l}(u_j - u_l)$ are now given in terms of elliptic functions. At $t = t_c = 1$ these elliptic functions become hyperbolic functions, with

$$B_{j,l} = -\exp\left(-i\Theta(u_j - u_l)\right) = -i\tanh(u_l - u_j - i\pi/4). \tag{A.1}$$

In terms of the variables u the quasimomenta $k(u)$ and the factors $e(u)$ in (51) are given by

$$k(u) = i/2 \ln\left(\frac{\tanh(i\pi/8 + u)}{\tanh(i\pi/8 - u)}\right), \tag{A.2}$$

$$e(u) = 1/2 \ln\left(\frac{\cosh(2u) + \sqrt{2}/2}{\cosh(2u) - \sqrt{2}/2}\right). \tag{A.3}$$

The Bethe-ansatz equations (46) or (52) can be written as

$$\frac{I_j}{N} = \frac{1}{2\pi}\left\{k(u_j) + \frac{1}{N}\sum_{l=1}^{n}\Theta(u_j - u_l)\right\} \quad j = 1, 2, ...n, \tag{A.4}$$

where $2I_j$ are integers or half-odd integers depending on the value of ϵ. The values of I_j for the lowest eigenenergy in the sector with given values of n and ϵ, which we are interested in, are

$$I_1, I_2, ..., I_n = -\frac{n-1-\tilde{\epsilon}}{2}, \frac{n-1-\tilde{\epsilon}}{2} + 1, ..., \frac{n-1+\tilde{\epsilon}}{2}, \quad \tilde{\epsilon} = \frac{1-\epsilon}{4}. \tag{A.5}$$

22

Following a standard procedure [19] we define the density of roots

$$\sigma_N^n(u) = \frac{dZ_N^n}{du}, \tag{A.6}$$

where

$$Z_N^n(u) = \frac{1}{2\pi} \left\{ k(u) + \frac{1}{N} \sum_{l=1}^{n} \Theta(u - u_l) \right\}. \tag{A.7}$$

When $N \to \infty$ (A.6) becomes an integral equation whose solution gives the bulk limit of the density of roots. In particular, in the sector $n = N$ this density of roots is given by

$$\sigma_\infty(u) = \frac{4}{\pi} \frac{\cosh(4u) \cosh(8u/3)}{\cosh(8u) + 1}. \tag{A.8}$$

In this limit the energy per site is given by [3]

$$e_\infty^{SCP} = -\frac{3}{4} \ln(6). \tag{A.9}$$

The difference between the energy per site and the density of roots and their bulk-limit values can be expressed by

$$\frac{E_N^n}{N} - e_\infty^{SCP} = -\int_{-\infty}^{\infty} f(v)S(v)dv, \tag{A.10}$$

and

$$\sigma_N^n(u) - \sigma_\infty(u) = -\frac{1}{2\pi} \int_{-\infty}^{\infty} p(u - v)S(v)dv, \tag{A.11}$$

respectively, where

$$S(v) = \frac{1}{N} \sum_{j=1}^{n} \delta(v - u_j) - \sigma_N^n(v), \tag{A.12}$$

$$p(u) = -\frac{8\sqrt{3}}{3} \frac{\sinh(8u/3)}{\sinh(4u)}, \tag{A.13}$$

$$f(u) = 1/2 \int_{-\infty}^{\infty} \frac{\sinh(\pi x/8)}{x \left(\cosh(\pi x/4) - 1/2 \right)} \exp(ixu)dx. \tag{A.14}$$

Using the Euler-Maclaurin formula we can expand (A.10) and (A.11), obtaining

$$\frac{E_N^n}{N} - e_\infty^{SCP} = \left(\int_{\Lambda_+}^{\infty} f(v)\sigma_N^n(v)dv - \frac{1}{2N}f(\Lambda_+) - \frac{1}{12N^2} \frac{f'(\Lambda_+)}{\sigma_N^n(\Lambda_+)} \right)$$
$$+ \left(\int_{\Lambda_-}^{\infty} \frac{f(v)}{2\pi}\sigma_N^n(v)dv - \frac{1}{2N}f(\Lambda_-) - \frac{1}{12N^2} \frac{f'(\Lambda_-)}{\sigma_N^n(\Lambda_-)} \right), \tag{A.15}$$

and

$$\sigma_N^n(u) - \sigma_\infty(u) = \left(\int_{\Lambda_+}^\infty \frac{p(u-v)}{2\pi} \sigma_N^n(v) dv - \frac{1}{2N} p(u - \Lambda_+) + \frac{1}{12N^2} \frac{p'(u-\Lambda_+)}{\sigma_N^n(\Lambda_+)} \right)$$

$$+ \left(\int_{\Lambda_-}^\infty \frac{p(u+v)}{2\pi} \sigma_N^n(v) dv - \frac{1}{2N} p(u + \Lambda_-) - \frac{1}{12N^2} \frac{p'(u+\Lambda_-)}{\sigma_N^n(\Lambda_-)} \right), \qquad (A.16)$$

respectively. In the above equations Λ_+ and Λ_- are the largest and smallest root determined by the condition

$$\int_{\Lambda_\pm}^\infty \sigma_N^n(u) du = \frac{1}{2N} \left(1 + \beta_\pm(n) \right), \qquad (A.17)$$

where

$$\beta_\pm(n) = \frac{N-n}{2} \mp \frac{1-\epsilon}{4}.$$

We should now consider separately the cases $u > \Lambda_+$ and $u < -\Lambda_-$. In the case where $u > \Lambda_+(u < -\Lambda_-)$ the corrections of $O(1/N^2)$ are calculated by neglecting the terms in the second (first), large bracket in (A.16). Defining

$$g(u) = p(u)/2\pi, \quad f^\pm(u) = \sigma_\infty(u + \Lambda_\pm), \quad \chi^\pm(u) = \sigma_N^n(u + \Lambda_\pm), \qquad (A.18)$$

we can write (A.16) as

$$\chi^\pm(t^\pm) - f^\pm(t^\pm) = \int_0^\infty g(t^\pm - v)\chi^\pm(v) dv - \frac{1}{2N} g(t^\pm) + \frac{1}{12N^2} \frac{g'(t^\pm)}{\sigma_N^n(\Lambda_\pm)}. \quad (A.19)$$

This is precisely the standard form of the Wiener-Hopf equation (see, for example Morse and Feshbach [16]). Its solution is obtained on defining the Fourier transforms

$$\tilde{\chi}_\pm^\pm(w) = \int_{-\infty}^\infty \exp(iwt)\chi_\pm^\pm(t) dt \qquad \chi_\pm^\pm(t) = \begin{cases} \chi^\pm(t) & t \gtrless 0 \\ \\ 0 & t \lessgtr 0 \end{cases} \qquad (A.20)$$

and the corresponding Fourier pairs $g \leftrightarrow \tilde{g}$, $f \leftrightarrow \tilde{f}$. Using the fact that

$$(1 - \tilde{g}(w))^{-1} = G_+(w)G_-(w), \qquad (A.21)$$

where

$$G_+(w) = \frac{\sqrt{2\pi}\Gamma(1/2 - iw/4)\exp(iw\ln(2)/4)}{\Gamma(5/6 - iw/8)\Gamma(1/6 - iw/8)} = G_-(-w), \qquad (A.22)$$

24

we can express $\tilde{\chi}_\pm^\pm(w)$, after some algebraic manipulations as

$$\tilde{\chi}_+^\pm(w) = C^\pm(w) + G_+(w)(Q_+^\pm + P^\pm(w)), \qquad (A.23)$$

where

$$C^\pm(w) = \frac{1}{2N} + \frac{iw}{12N^2\sigma_N^n(\Lambda_\pm)} \qquad Q_+^\pm(w) = \frac{2}{\pi}\frac{G_+(i4/3)\exp(-4/3\Lambda_\pm)}{4/3 - iw}, \qquad (A.24)$$

$$P^\pm(w) = -\frac{1}{2N} + \frac{i(g_1 - w)}{12N^2\sigma_N^n(\Lambda_\pm)} \qquad g_1 = 109/6. \qquad (A.25)$$

Equations (A.19) and the definitions (A.18) give us

$$Q_+^\pm(0) = \frac{3}{2\pi}G_+(i4/3)\exp(-4/3\Lambda_\pm) = \frac{1}{2N} - \frac{ig_1}{12N^2\sigma_N^n(\Lambda_\pm)} + \frac{1}{2N}\frac{\beta_\pm}{G_+(0)}, \qquad (A.26)$$

$$\sigma_N^n(\Lambda_\pm) = \frac{g_1^2/2 - 4/3ig_1}{12N^2\sigma_N^n(\Lambda_\pm)} + \frac{ig_1 + 4/3}{2N} + \frac{4/3\beta_\pm(n)}{2NG_+(0)}. \qquad (A.27)$$

Finally, using (A.23),(A.26) and (A.27) in (A.15) and approximating $f(|u|) = \sqrt{3}\exp(-4/3|u|)$, $u \gg 1$, we obtain the first-order correction for the lowest energy $E_N^{n,\epsilon} = E_N^{(n)}$ in the sector with n dislocations and colour parity ϵ,

$$\frac{E_N^n}{N} - e_\infty^{SCP} = \frac{\pi v_s^{SCP}}{6N^2}(-1/6 + 2X_r^\epsilon) + o(1/N^2), \qquad (A.28)$$

where

$$X_n^\epsilon = \frac{(N-n)^2}{8} + \frac{(1-\epsilon)^2}{16}. \qquad (A.29)$$

In particular for the ground-state energy $n = N$, $\epsilon = 1$, we have

$$\frac{E_N^0}{N} \equiv \frac{E_N^{N,+}}{N} = e_\infty^{SCP} - \frac{\pi v_s^{SCP}}{6N^2} + o(1/N^2), \qquad (A.30)$$

and comparing with (47) we obtain the value $c = 1$ for the conformal anomaly. If we now consider the gaps with respect to the ground-state with periodic boundary condition we obtain

$$\frac{E_N^{N,\epsilon}}{N} - \frac{E_N^0}{N} = \frac{2\pi v_s^{SCP}X_n^\epsilon}{N^2} + o(1/N^2).$$

Comparing this expression with (48) we obtain the conformal dimensions X_n^ϵ. These values are in perfect agreement with the operator content conjectured for the SCP and Baxter-Wu model, presented in section 4.

References

[1] Wood D W and Griffiths H P 1972 *A self dual relation for an Ising model with triplet interactions J. Phys. C* **5** L253

[2] Merlini D and Gruber C 1972 *Spin-1/2 lattice system: Group structure and duality relation J. Math. Phys.* **13** 1814

[3] Baxter R J and Wu F Y 1973 *Exact Solution of an Ising model with three-spin interaction on a triangular laticce Phys. Rev. Lett.* **31** 1294; *Ising model on a triangular lattice with three-spin interaction. I The eigenvalue equation Aust. J. Phys.* 1974 **27** 357; Baxter R J 1974 *Ising model on a triangular lattice with three-spin interaction. II Free energy and correlation length Aust. J. Phys.* **27** 369 357

[4] Domany E and Riedel E K 1978 *Phase-transitions in 2-dimensional systems J. App. Phys.* **49** (3) 1315

[5] Wu F Y 1982 *The Potts-model Rev. Mod. Phys.* **54** 235

[6] Baxter R J 1982 *Exactly Solved Models in Statistical Mechanics* (New York : Academic)

[7] Cardy J L 1986 *Logarithmic corrections to finite-size scaling in strips J. Phys. A: Math. Gen* **19** L1093

[8] Alcaraz F C, Barber M N and Batchelor M T 1987 *Conformal-Invariance and the spectrum of the XXZ chain Phys. Rev.Lett.* **58** 771; 1988 *Conformal-Invariance, the XXZ chain and the operator content of two-dimensional critical systems Ann. Phys.* (NY) **182** 280

[9] Hamer C J, Batchelor M T and Barber M N 1988 *Logarithmic corrections to finite-size scaling in the 4-states Potts-model J. Stat. Phys.* **52** 679

[10] Hamer C J 1981 *Q-State Potts models in hamiltonian field-theory for* $Q \geq 4$ *in (1+1) dimensions J. Phys. A: Math. Gen.* **14** 2981

[11] Barber M N 1985 *Phenomenological renormalization of multi-parametere systems Physica* **130A** 171

[12] Alcaraz F C and Xavier J C 1997 *Conformal invariance studies of the Baxter-Wu model and a related site-colouring problem J. Phys. A: Math. Gen.* **30** L203

[13] See, e.g., Cardy J L 1986 *Phase Transitions and Critical Phenomena* vol. 11, ed. C Domb and J L Lebowitz (New York:Academic)

[14] Baake M, Gehlen G v and Rittenberg V 1987 *Operator content of the Ashkin-Teller quantum chain - Superconformal and Zamolodchikov-Fateev invariance - I - Free-Boundary conditions* it J. Phys. A: Math. Gen. **20** L479 and *O Operator content of the Ashkin-Teller quantum chain - Superconformal and Zamolodchikov-Fateev invariance - II Boundary-Conditons compatible with the torus* J. Phys. A: Math. Gen. **20** L487

[15] Ginsparg P 1990 *Fields, Strings and Critical Phenomena* Les Houches XLIX, p. 1, eds. E. Brézin and J. Zinn-Justin (North Holland, Amsterdam)

[16] Morse P M and Feshbach H 1953 *Methods of Theoretical Physics*, (New York: McGraw-Hill) p 978

[17] Blöte H, Cardy J L and Nightingale M 1986 *Conformal-Invariance, the central charge, and universal finite-size amplitudes at criticality* Phys. Rev. Lett. **56** 742; Affleck I 1986 *Universal term in the free-energy at a critical-point and the conformal anomaly Phys. Rev. Lett.* **56** 746

[18] Cardy J L 1986 *Operator content of two-dimensional conformally invariant theories Nucl. Phys. B* **270** 186

[19] de Vega H and Woynarovich F 1985 *Method for calculating finite size corrections in the Bethe ansatz systems - Heisenberg chain and 6-Vertex model Nucl. Phys. B* **251** [FS13]

[20] Hamer C J 1986 *Finite-size corrections for ground-states of the XXZ Heisenberg chain J. Phys. A: Math. Gen.* **19** 3335

[21] Woynarovich F and Eckle H P 1987 *Finite-size corrections and numerical-calculations for long spin-1/2 Heisenberg-chains in the critical region J. Phys. A: Math. Gen.* **20** L97

[22] Hamer C J, Quispel G R W and Batchelor M T 1987 *Conformal anomaly and surface-energy for Potts and Ashkin-Teller quantum chains J. Phys. A: Math. Gen.* **20** 5677

[23] Sagdeev I R and Zamolodchikov A B 1989 *Numerical check of the exact mass spectrum of the scaling limit of T_c Ising model with magnetic field Mod Phys. Lett. B* **3** 1375

[24] Henkel M and Saleur A 1990 *Remarks on the mass-spectrum on noncritical coset models from Toda theories J. Phys. A: Math. Gen.* , **23** 791

[25] Dashen RF, Hasslacher B and Neveu A 1975 *Particle spectrum in model field-theories from semiclassical functional integral techniques Phys. Rev. D* **11** 3424 ; Zamolodchicov A B and Zamolodchicov A B 1979 *Factorized S-matrices in 2 dimensions as the exact solutions of certain relativistic quantum field-theory models Ann. Phys.* (NY) **121**

[26] Henkel M and Ludwig A W W 1990 *Mass-Spectrum of the 2D Ashkin-Teller model in an external magnetic-field Phys. Lett. B* **249** 463

[27] Kadanoff L P and Brown A C 1979 *Correlation-Funcions on the critical lines of the Baxter and Ashkin-Teller models Ann. Phys.* (NY) **121** 318

Figure and Table Captions

Figure 1 - A triangular lattice with $L = 3$ rows and $M=6$ columns. The Baxter-Wu model is defined on the triangular lattice formed by the points ○, □ and △, and the link variables $\{\lambda\}$ are defined on the hexagonal lattice formed by the points □ and ○. The site-colouring problem (SCP) is defined on the hexagonal lattice formed by the points △ and ○. The open symbols ○, □ and △ denote the bordering sites related through (2) with the bulk ones (filled simbols).

Figure 2 - Examples of configurations for the SCP with lattice size $N = 4$. The dislocations are represented by dotted lines. In (a) the configurations $(m; X) = (1; 2, 3, 4, 4)$ and $(m'; X') = (3; 2, 2, 3, 4)$ are in the sector $n = 4$ $(\kappa = 0)$. In (b) the configurations $(m; X) = (1; 2, 3, 4)$ and $(m'; X') = (3; 2, 2, 2)$ belong to the sector $n = 3$ $(\kappa = 1)$.

Table 1 - Ground-state energies per site for the SCP with lattice size N and boundary conditions $\kappa = 0, 1$ and 2 given by (15).

Table 2 - Conformal anomaly estimators $c(N)$, as a function of the lattice size N, for the SCP and Baxter-Wu model.

Table 3 - Scaling dimensions estimators $x_j^\epsilon(N - n, l)$, as a function of the lattice size N, for some eigenenergies. These energies are the jth lowest energy obtained by solving (50)-(52) with values n, ϵ and l.

Table 4 - Energies for the Baxter-Wu model and SCP. The energies of the same line are identical.

Table 5 - The mass-ratio estimators $R_2(X, L)$ defined in (60).

Table 6 - The mass-ratio estimators $R_3(X, L)$ defined in (60).

Table 1

N	$\kappa = 0$	$\kappa = 1$	$\kappa = 2$
6	-1.3521881950	-1.3396181681	-1.3012024788
10	-1.3468393066	-1.3423074850	-1.3286264987
50	-1.3439405169	-1.3437591407	-1.3432148801
100	-1.3438498316	-1.3438044868	-1.3436684443
150	-1.3438330374	-1.3438128841	-1.3437524226
200	-1.3438271593	-1.3438158231	-1.3437818139

Table 2

N	$c(N)$
6	0.996590995
10	0.998910268
50	0.999959561
100	0.999989915
150	0.999995519
200	0.999997480

Table 3

N	6	10	50	100	150	200	exact
$x_1^-(0,0)$	0.12502803	0.12501702	0.12500083	0.12500021	0.12500009	0.12500005	0.125
$x_2^-(1,0)$	0.24896741	0.24959771	0.24998323	0.24999580	0.24999813	0.24999895	0.25
$x_2^+(0,1)$	0.50626226	0.50215317	0.50008406	0.50002099	0.50000933	0.50000525	0.5
$x_1^-(2,0)$	0.62613504	0.62548322	0.62502093	0.62500524	0.62500233	0.62500131	0.625
$x_4^+(0,1)$	0.98648357	0.99698967	0.99992101	0.99998057	0.99999139	0.99999516	1
$x_1^+(3,0)$	1.16335432	1.13836199	1.12552520	1.12513123	1.12505831	1.12503280	1.125
$x_1^-(3,0)$	1.27059213	1.25887795	1.25038505	1.25009649	1.25004290	1.25002413	1.25
$x_6^+(0,2)$	1.53502476	1.51231634	1.50048724	1.50012177	1.50005411	1.50003044	1.5
$x_{10}^+(0,1)$	1.82581639	1.97119336	1.99980095	1.99995795	1.99998195	1.99998997	2

Table 4

BW	SCP
	$E_7^{SCP}(\epsilon = 1)$
E_3^{BW}	$E_6^{SCP}(\epsilon = -1)$
	$E_5^{SCP}(\epsilon = -1)$
E_2^{BW}	$E_4^{SCP}(\epsilon = 1)$
	$E_3^{SCP}(\epsilon = 1)$
E_1^{BW}	$E_2^{SCP}(\epsilon = -1)$
	$E_1^{SCP}(\epsilon = -1)$
E_0^{BW}	$E_0^{SCP}(\epsilon = 1)$

Table 5

X	m_2/m_1
2	1.4049
5	1.7169
6	1.7273
7	1.7303

Table 6

X	m_3/m_1
10	2.02632
20	2.00538
40	2.00123
40	2.00053
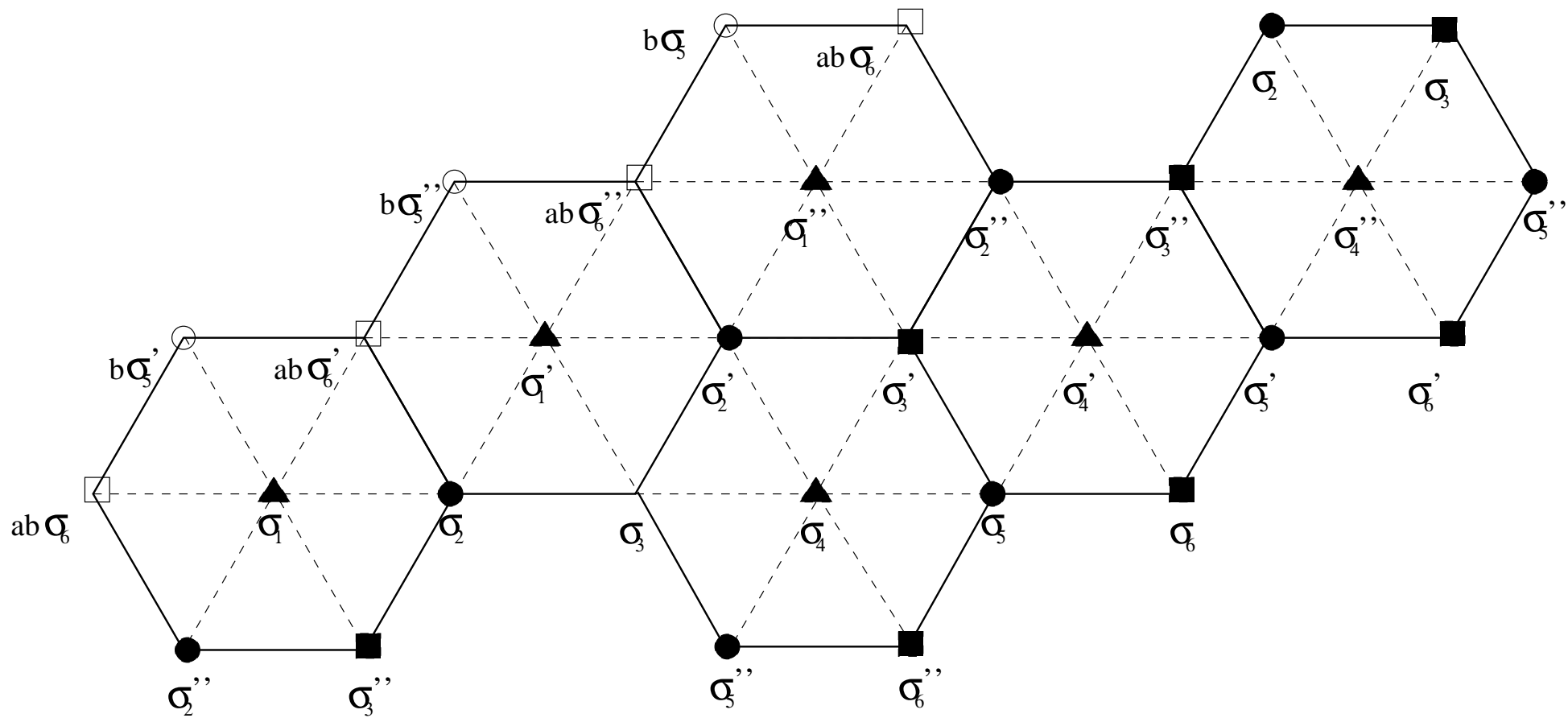
Fig. 1

$\{m',C'\}=(3;2,2,2)$

$\{m,C\}=(1;2,3,4)$

Fig.2b

$\{m',C'\}=(3;2,2,3,4)$

$\{m,C\}=(1;2,3,4,4)$

Fig.2a